

# Chemical synthesis of nanocrystalline CuAlO<sub>2</sub> via nitrate-citrate combustion route

Katarina Vojisavljević<sup>a</sup>, Biljana Stojanović<sup>b</sup>, Brigita Kmet<sup>a</sup>, Jena Cilenšek<sup>a</sup>, Barbara Malič<sup>a</sup>

<sup>a</sup> *Jožef Stefan Institute, Jamova cesta 39, 1000 Ljubljana, Slovenia*

<sup>b</sup> *Institute for Multidisciplinary Research, Kneza Višeslava 1, 11030 Belgrade, Serbia*

**Abstract:** The nanocrystalline delafossite CuAlO<sub>2</sub> powder was synthesised by a sol-gel nitrate-citrate self-combustion route. Citric acid was introduced both as the chelating and reducing agent or fuel. The citric acid/metal ion ratio was adjusted to provide fuel-lean, stoichiometric or fuel-rich conditions of the redox reaction. Equimolar amounts of copper and aluminium nitrates and the citric acid were dissolved in deionized water. The sol was dried at 80 °C to obtain the gel. By increasing the temperature above 250 °C, the gel immediately ignited, forming the precursor powder. According to the X-ray diffraction analysis the phase pure delafossite was obtained only when the precursor powder was prepared from the stoichiometric redox reaction, and after the calcination for 4 h in Ar atmosphere at 920 °C. The field emission scanning electron micrographs revealed the cauliflower aspect of the calcined powder, where small primary particles formed the agglomerates. The formation of the phase pure CuAlO<sub>2</sub> powder was also confirmed by Fourier transformed infrared spectroscopy.

**Key words:** delafossite, sol-gel citric-nitrate combustion synthesis, XRD, FE-SEM, FT-IR.

## 1 Introduction

Recently, a considerable effort has been devoted to research of the p-type semiconducting, narrow band gap CuAlO<sub>2</sub> material. The importance of this material lies in the fact that it can be used as a transparent conducting oxide (TCO) in the field of invisible electronics for production of different optoelectronic devices. However, scientists involved in investigation of CuAlO<sub>2</sub> are interested not only in examination of the TCOs properties, but also in exploring its applications as a catalyst for the conversion of solar power to hydrogen energy, room temperature ozone sensors, or thermoelectric devices. The performance of CuAlO<sub>2</sub> in some of the mentioned applications could be optimized by increasing surface area and decreasing its particle size. Therefore, the synthesis of nanocrystalline CuAlO<sub>2</sub> has been a hot and open topic for material chemists.

Up to now, different methods such as solid-state reaction [1-3], hydrothermal method [4], ion exchanges [5] etc. have been employed to prepare CuAlO<sub>2</sub>. Furthermore, the sol-gel method, where the citric acid was used as a chelating agent, was also proposed as a possible and useful method for the preparation of the nanocrystalline CuAlO<sub>2</sub> powders [6]. On the other side, the citric acid is also known as a good reducing agent, i.e. fuel for combustion synthesis of different oxide powders [7]. Combining the chelating/fuel properties of the citric acid, and using the propellant chemistry to adjust the amount of the citric acid to nitrate ions, the combustion of the citrate-nitrate sols could be usefully employed for production of nanocrystalline copper-aluminate powders. The fuel-to-oxidizer ratio relative to the stoichiometric fuel-to-oxidizer ratio, defined as the equivalence ratio ( $\phi$ ) was adjusted to provide fuel-lean, stoichiometric or fuel-rich conditions of the redox

reaction. In this work, we propose a simple method for preparation of the nanocrystalline  $\text{CuAlO}_2$  powders by self-sustained combustion synthesis route from the citrate-nitrate based solutions. The results of the synthesis and characterization of the  $\text{CuAlO}_2$  powder are discussed herein.

## 2 Materials and Methods

The precursor powders were synthesized by a two-step procedure including the preparation of a metal-citrate precursor and its thermal decomposition during the combustion. A clear solution was prepared by dissolving  $\text{Al}(\text{NO}_3)_3 \cdot x\text{H}_2\text{O}$  (Alfa Aesar, p.a. 99.999 %) and  $\text{Cu}(\text{NO}_3)_2 \cdot y\text{H}_2\text{O}$  (Alfa Aesar, p.a. 99.999 %) in a minimum amount of deionized water, taking into account the stoichiometric relationship between metal ions,  $\text{Cu}/\text{Al} = 1.0$ . Then, the citric acid (Alfa Aesar, anhydrous, p.a. 99.5 %) as the chelating-fuel agent was added to the solution. To find the proper amount of the citric acid, necessary for the complete combustion reaction, the oxidizer to fuel ratio (O/F) was calculated according to the rule of propellant chemistry, using the total valence of oxidizers (nitrates) and the reducing valence of the fuel (citric acid). The value of the calculated O/F ratio is 1.45. The experiments were performed in fuel-lean (equivalence ratio  $\phi = 0.69$ ), stoichiometric ( $\phi = 1$ ) and fuel-rich ( $\phi = 1.385$ ) conditions, meaning that the molar ration of the citric acid/metal ions were adjusted to be 1, 1.45 and 2, respectively. The solutions were agitated at room temperature for 1 h, and then neutralized to increase the efficiency of the chelating agent by adding ammonia (25%) drop-wise. The concentration of the resultant sols was close to 0.2 M. The sols were continuously stirred at  $60\text{ }^\circ\text{C} - 80\text{ }^\circ\text{C}$  for several hours to evaporate the water and increase the viscosity. In this step, the color was changed from light-blue to deep-blue, while the sols were turned to homogeneous gels. During the rapid heating to  $500\text{ }^\circ\text{C}$ , the gels auto-ignited at approximately  $250\text{ }^\circ\text{C}$  (depending on the amount of the fuel) and underwent smouldering combustion spontaneously with the evolution of large amounts of gases, subsequently forming the gray-black voluminous precursor powders. The obtained precursor powders were ground in a mortar, uniaxially pressed into pellets with 50 MPa and heat-treated at  $920\text{ }^\circ\text{C}$  for 4 h in argon atmosphere. The rate of the heating and cooling cycles was set to  $5\text{ }^\circ\text{C}/\text{min}$ . For clarity purpose, the sols, the precursor powders and the heat treated powders were named herein by the sol, combustion and heat treatment acronym followed by the equivalence ratio,  $\phi$  between brackets, e.g. S(0.69), C(0.69) and HT(0.69).

The samples of precursors and precursor sols were analysed by thermogravimetric and differential thermal analysis (TG/DTA, NETZSCH STA 409) in flowing air atmosphere with the heating rates of 2 or  $10\text{ }^\circ\text{C}/\text{min}$ . The morphology of the powders was examined by the field emission scanning electron microscope FE-SEM (JEOL JSM 7600F, Tokyo, Japan). The particle sizes, expressed as the median value ( $d_{50}$ ), and size distributions (PSD) of the powders were determined from the area distributions measured by a laser granulometer (Microtrac S3500 Particle Size Analyzer, Montgomeryville, PA). The surface area was analyzed using the  $\text{N}_2$  adsorption BET method (NOVA 2200E, Quantachrome Instruments, Boynton Beach, FL, USA). Before the analysis the samples were degassed at  $100\text{ }^\circ\text{C}$  under  $0.04\text{ }\mu\text{mHg}$  pressure during 1 h to remove traces of water and adsorbed gases. The phase composition of the powders was analysed by PANalytical diffractometer (X'Pert PRO MPD, Almelo, Netherlands, Bragg-Brentano geometry using the  $\text{CuK}\alpha$  radiation and X'Celerator detector configured in reflection geometry). The data acquisition was done in the step scan mode ( $2\theta = 0.034^\circ$ , integration time 100 s) in angular range  $2\theta = 10 - 70^\circ$ . The phases were identified with the X'Pert High Score package, using the PDF-2 reference patterns database. The crystallite size of the  $\text{CuAlO}_2$  powder was calculated using the Debye-Scherrer equation (Eq. (1)):

$$L = \frac{k\lambda}{\beta(2\theta)\cos\theta} \quad (1)$$

where  $L$  is the crystallite size,  $\lambda$  the wavelength ( $\text{CuK}\alpha_1$ ,  $0.15406\text{ nm}$ ),  $k$  the dimensionless shape factor ( $= 0.94$ ),  $\theta$  the Bragg angle. The half-width of the diffraction line  $\beta(2\theta)$  in radians was taken as the experimental half-width ( $\beta_{\text{exp.}}$ ) and was corrected for experimental broadening ( $\beta_{\text{ins.}}$ ) according to:

$$\beta(2\theta) = \left( \beta_{\text{exp.}}^2 - \beta_{\text{ins.}}^2 \right)^{1/2} \quad (2)$$

The  $\beta_{\text{ins}}$  was measured experimentally by a highly crystalline  $\text{LaB}_6$  powder.

Fourier Transform Infrared spectra were recorded by a Perkin Elmer Spectrum 100 spectrometer in an attenuated total reflectance (ATR) mode. The resolution was set at  $4\text{ cm}^{-1}$  in the spectral range covering  $4,000\text{--}400\text{ cm}^{-1}$ .

### 3 Results

First, the thermal decomposition pathways of the  $\text{Al}(\text{NO}_3)_3 \cdot x\text{H}_2\text{O}$  and  $\text{Cu}(\text{NO}_3)_2 \cdot y\text{H}_2\text{O}$  were analysed by TG-DTA, see Fig. 1. Upon heating of the  $\text{Al}(\text{NO}_3)_3 \cdot x\text{H}_2\text{O}$  to  $500\text{ }^\circ\text{C}$  in air (Fig. 1 a) the total weight loss of 83.63 % is recorded. The dehydration of the salt corresponds to endothermic peaks at  $101\text{ }^\circ\text{C}$  and  $121\text{ }^\circ\text{C}$ , and is directly followed by the decomposition of the aluminium nitrate coupled with two endothermic events at  $174\text{ }^\circ\text{C}$  and  $189\text{ }^\circ\text{C}$ . According to DTA, the reaction ends at approximately  $200\text{ }^\circ\text{C}$ , but the TG result indicates the slow release of the nitrogen gas species ( $\text{N}_2$ ,  $\text{NO}$ ,  $\text{NO}_2$ ) up to  $400\text{ }^\circ\text{C}$ . The total weight loss upon heating of the  $\text{Cu}(\text{NO}_3)_2 \cdot y\text{H}_2\text{O}$  from room temperature to  $500\text{ }^\circ\text{C}$  is 68.15 %, see Fig. 1 b). It decomposes within two distinct steps. The first step ( $100\text{--}225\text{ }^\circ\text{C}$ ) with the weight loss of 37 % is mainly attributed to the removal of the physisorbed water and is accompanied with two endothermic peaks at  $133\text{ }^\circ\text{C}$  and  $183\text{ }^\circ\text{C}$ . The second step ( $225\text{--}300\text{ }^\circ\text{C}$ ) with the weight loss of 31.15 %, coupled with an endothermic event at  $270\text{ }^\circ\text{C}$  is related to the decomposition of the nitrate to  $\text{CuO}$ . Based on the TG-DTA result, the calculated molar masses of the copper and aluminium nitrate salts are  $249.729\text{ g/mol}$  and  $417.531\text{ g/mol}$ , respectively and thus the compounds can be described as  $\text{Cu}(\text{NO}_3)_2 \cdot 3.45\text{H}_2\text{O}$  and  $\text{Al}(\text{NO}_3)_3 \cdot 11.35\text{H}_2\text{O}$ .

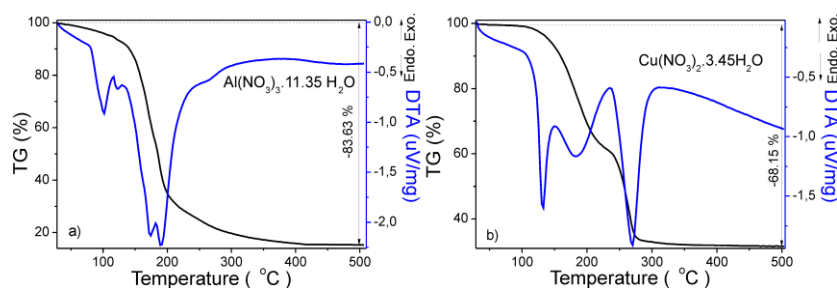
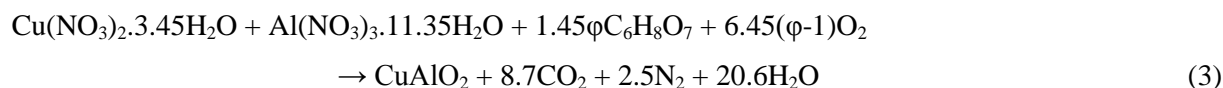


**Figure 1:** TG-DTA of the a)  $\text{Al}(\text{NO}_3)_3 \cdot x\text{H}_2\text{O}$  and b)  $\text{Cu}(\text{NO}_3)_2 \cdot y\text{H}_2\text{O}$  in air with the heating rate of  $10\text{ }^\circ\text{C/min}$ .

Assuming the complete combustion, the equation for the formation of the copper-aluminate in the presence of the citric acid is written as follows (Eq. (3)):



where the  $\varphi$  is the fuel-to-oxidizer equivalence ratio, set to be 0.69 - for the fuel-lean, 1 - for the stoichiometric and 1.385 - for the fuel-rich conditions. Only in the case of the stoichiometric mixture, ( $\varphi = 1$ ) the oxygen does not participate in the reaction. In the fuel-lean conditions, the excess oxygen appears in the exhaust gas, while the atmospheric oxygen would be needed for the completion of the fuel-rich reaction. The experimental observation showed that the sols with all oxidizer to fuel ratios exhibited the self-propagation combustion behavior. The ignition of the dried gels occurred at approximately  $250\text{ }^\circ\text{C}$ . All mixtures underwent the smouldering combustion with the formation of a large amount of gases, but the most intense reaction occurred in the case of the stoichiometric oxidizer to fuel ratio.

The thermal decomposition of the citrate based sols was investigated by the TG-DTA analysis. The decomposition undergoes in several steps (Fig. 2). The two endothermic effects in the temperature range  $106\text{--}122\text{ }^\circ\text{C}$  could be assigned to water loss, while the first exothermic peak at  $224\text{ }^\circ\text{C}$  for the stoichiometric redox composition, and at a bit higher temperatures,  $\sim 228\text{ }^\circ\text{C}$  and  $\sim 233\text{ }^\circ\text{C}$ , for the fuel-lean,  $S(0.69)$ , and fuel-rich compositions,  $S(1.385)$ , respectively, indicated a complete and fast decomposition due to the combustion of the nitrates and citrates. The second endothermic event in the temperature range  $273\text{--}359\text{ }^\circ\text{C}$  could be related to the release of gases due to oxidation of the carbon

residues, and crystallization. According to DTA results, see the inset in Fig. 2, the exothermicity of the precursor mixture S(1) was the most pronounced and it decreased for both non-stoichiometric precursor mixtures, S(0.69) and S(1.385). The exothermicity, or the energy released by the combustion of the redox mixtures strongly depends on the oxidizer-to-fuel ratio and it is at its maximum when the equivalence ratio,  $\phi$  is unit. Otherwise, the amount of the nitrate ions (oxidant) are in excess (S(0.69), fuel-lean condition) or insufficient (S(1.385), fuel-rich condition) for the oxidation of the citrate ions in the redox mixture, and the combustion is incomplete. This can explain the decrease of the exothermicity for the S(0.69) and S(1.385) mixtures.

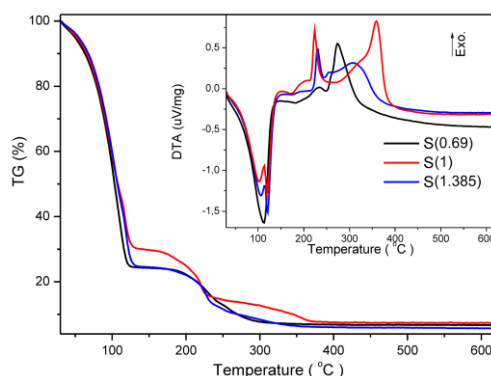


**Figure 2:** TG and DTA (inset) of the a) S(0.69), b) S(1) and c) S(1.385) in air at heating rate of the 2 °C/min.

The X-ray diffraction patterns of the as-combusted powders C(0.69), C(1) and C(1.385) are shown in Fig. 3. The results indicate that the as-prepared powders were mixtures of the amorphous matrix and crystalline monoclinic CuO phase (PDF 01-089-5897, space group: C2/c). Besides the CuO, a small amount of the crystalline cubic Cu<sub>2</sub>O phase (PDF 01-078-2076, space group: Pn-3m) was also found in the combusted C(1) and C(1.385) powders. The unidentified peak at 44.416° in the XRD patterns of the C(1) and C(1.385) powders could be due to the formation of one of the transient alumina phases ( $\eta$ -Al<sub>2</sub>O<sub>3</sub>,  $\gamma$ -Al<sub>2</sub>O<sub>3</sub>,  $\delta$ -Al<sub>2</sub>O<sub>3</sub>,  $\theta$ -Al<sub>2</sub>O<sub>3</sub>). Broad diffraction peaks of the Cu<sub>2</sub>O and Al<sub>2</sub>O<sub>3</sub> indicate the low crystallinity and possibly the presence of the amorphous phase. The crystallite size of the CuO in the combusted powders was calculated from the broadening of the CuO reflections using the Debye–Scherrer equation (Eq. (1)). It was found that the crystallite sizes of the CuO in the C(0.69), C(1) and C(1.385) specimens are 32.3 nm, 36 nm and 35.8 nm, respectively. Larger crystallites were present in the C(1) and C(1.385) samples.

The combusted powders were calcined in argon atmosphere at 920 °C. The calcination conditions were selected on the basis of the results obtained for the combusted-powder compacts in a heating stage microscope (not presented here). The calcination of the C(1) powder at 920 °C for 4h resulted in the formation of the single-phase delafossite, while in the case of the C(0.69) and C(1.385) samples secondary phases were also present. Therefore, the HT(1) was considered for further analysis.

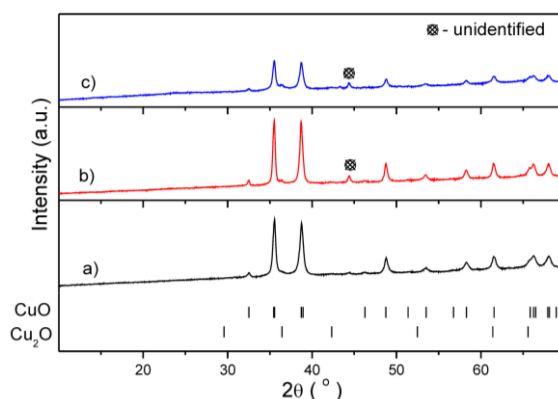


**Figure 3:** XRD patterns of the as-combusted a) C(0.69) and b) C(1) and c) C(1.385) powders.

FE-SEM revealed the cauliflower aspect of the HT(1) powder, where the plate-like particles of a few 100 nm in size form agglomerates with the average size of 5 to 10  $\mu\text{m}$  and a large number of pores and voids, see Fig. 4 a). The specific surface area of the C(1) powder, before calcination was 13.735  $\text{m}^2/\text{g}$ , while this value was changed to 9.075  $\text{m}^2/\text{g}$  after the heat treatment at 920  $^\circ\text{C}$  for 4 h. The granulometric result indicates that the median particle size ( $d_{50}$ ) of the HT(1) powder is 2.172  $\mu\text{m}$  and 90% of the particles ( $d_{90}$ ) are smaller than 11.03  $\mu\text{m}$  (Fig. 4b). The XRD pattern (Fig. 4c) of the crystalline product revealed that it contains only rhombohedral  $\text{CuAlO}_2$  (PDF 00-035-1401, space group: R-3m) phase, with the crystallite size of 24 nm according to Debye–Scherrer equation, as already explained above.

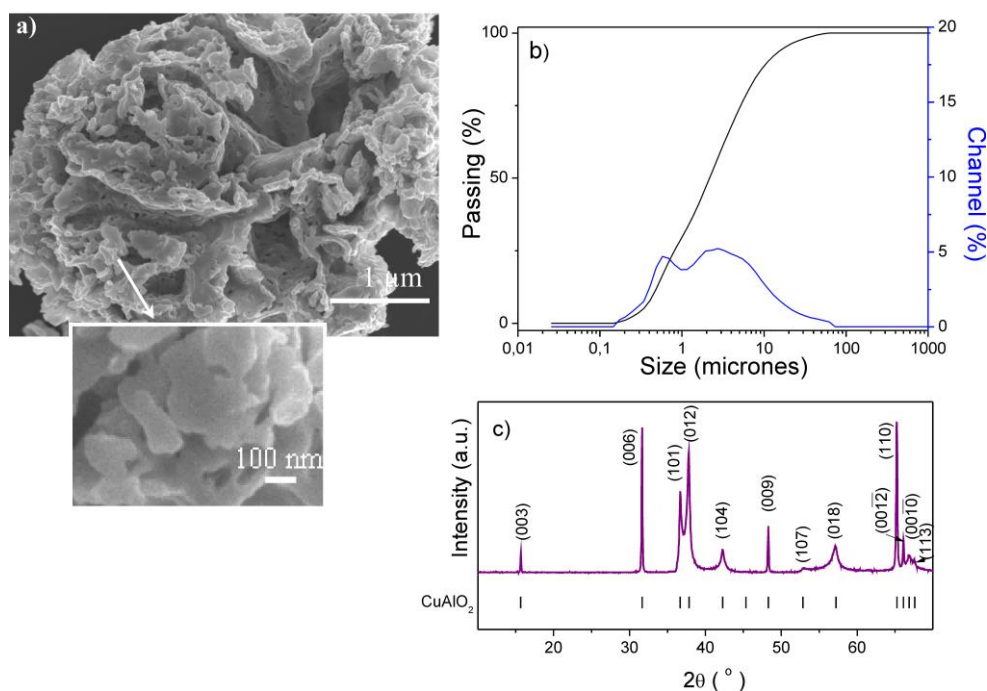


**Figure 4:** HT(1) powder thermally treated at 920  $^\circ\text{C}$  in argon: FE-SEM a), PSD b) and XRD pattern c).

The formation of the delafossite phase from the S(1) solution to the delafossite HT(1) powder was also analysed by FT-IR spectroscopy and the results are shown in Fig. 5), along with the FT-IR spectrum of the citric acid. The broad band centred around 3300  $\text{cm}^{-1}$  in the spectrum of the S(1) sol is due to the O-H stretching vibration of water. After gelation, the COO-H stretching vibration (3198  $\text{cm}^{-1}$ ) and C-H symmetric/anti-symmetric stretching vibrations (3032  $\text{cm}^{-1}$  and 2841  $\text{cm}^{-1}$ ) appear in the spectrum of the S(1) gel precursor. Upon comparison of the FT-IR spectra of the citrate-based sol and gel precursors with the spectrum of the citric acid, the shifts of the intense bands from 1697  $\text{cm}^{-1}$  and 1427  $\text{cm}^{-1}$  are evident. They can be related to the C=O stretching vibration of the carboxylate groups at 1563  $\text{cm}^{-1}$  and 1310  $\text{cm}^{-1}$ , indicating the coordinative bonding of the citrate ligand to the metal ions. The band located at 1071  $\text{cm}^{-1}$  could be assigned to the C—O stretching of the deprotonated alcohol group of the ligand [8], while the presence of the NO stretching vibration from the nitrate group is confirmed by the bands at 1043  $\text{cm}^{-1}$  and 828  $\text{cm}^{-1}$ . The bands related to the C—C stretching are in the region 959 – 902  $\text{cm}^{-1}$ , and the rocking mode of the  $\text{CH}_2$  group is located at 864  $\text{cm}^{-1}$ . The spectrum of the S(1) gel precursor presents the characteristic bands of the coordinated water at 3470  $\text{cm}^{-1}$  and 631  $\text{cm}^{-1}$ . The modes below 800  $\text{cm}^{-1}$  probably include vibrational modes of the water, and Al—O and Cu—O motions. In the spectrum of the combusted powder the bands related to organic groups disappear, while those related to the Cu—O and Al—O motions become evident. The strong and sharp bands in the HT(1) spectrum at 935, 726 arise from the Al—O stretching vibration in distorted  $\text{AlO}_6$  octahedra, while the band at 481  $\text{cm}^{-1}$  is due to the Cu—O stretching vibration. Such vibrations are typical for the layered  $\text{CuAlO}_2$  structure [6].

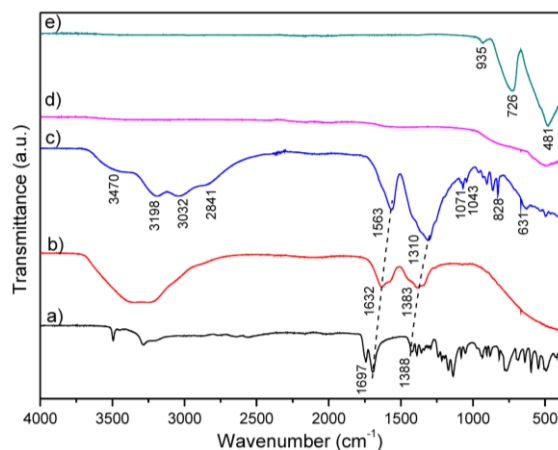


**Figure 5:** FTIR spectra of the a) citric acid, b) S(1) sol precursor, c) S(1) gel precursor, d) C(1) and e) HT(1).

The presence of the coordinated water in the gel, observed by FT-IR, could decrease the temperature of the system during the combustion and possibly hinder the formation of the  $\text{CuAlO}_2$ . Nevertheless, the pure  $\text{CuAlO}_2$  powder was obtained after calcination at  $920\text{ }^\circ\text{C}$  for 4h in argon. Compared with the solid state synthesis where high processing temperatures ( $1100\text{ }^\circ\text{C}$ ) and long reaction times (96 h) have been used to obtain single-phase delafossite  $\text{CuAlO}_2$  [1, 2], both the calcination temperature and the dwell time are certainly lowered by the proposed citrate-nitrate combustion route.

## 4 Conclusions

The self-sustained nitrate-citrate combustion route has been employed for the preparation of the oxide-precursor powder. The double role of the citric acid, as the chelating agent and the fuel, was of great importance in preventing the precipitation from the solution in the course of the reaction with the changing pH, and in liberation of the required energy for the synthesis of the precursor powder in the redox reaction with the nitrate ions. According to XRD, phase-pure  $\text{CuAlO}_2$  was obtained after calcination of the precursor powder at  $920\text{ }^\circ\text{C}$  for 4 h in argon, which is significantly less than  $1100\text{ }^\circ\text{C}$  for the solid state reaction. Nanocrystallites of 24 nm in size form the plate-like particles and agglomerates with a cauliflower aspect and a large number of pores. The proposed method results in a high specific surface area of the powder -  $9.075\text{ m}^2/\text{g}$ .

## 5 Acknowledgments

We acknowledge the financial support of the Slovenian research agency (research programme P2-0105 and projects J2-4273) and the EC within the 7FP ORAMA project: Oxide materials for electronics applications, Grant Agreement NMP3-LA-2010-246334.

## 6 References

- [1] Y. C. Liou, U. R/ Lee, Non-calcining process for  $\text{CuAlO}_2$  and  $\text{CuAl}_{0.9}\text{Ca}_{0.1}\text{O}_2$  ceramics. *J. Alloys Comp.* 2009;**467**:496-500.
- [2] X. G. Zheng, K. Taniguchi, A. Takahashi, Y. Liu, C. N. Xu, Room temperature sensing of ozone by transparent p-type semiconductor  $\text{CuAlO}_2$ . *Appl. Phys. Lett.* 2004;**85**:1728-9.
- [3] K. Vojisavljević et al., Solid state synthesis of nano-boehmite-derived  $\text{CuAlO}_2$  powder and processing of the Ceramics, *J Eur Ceram Soc* (2013), <http://dx.doi.org/10.1016/j.jeurceramsoc.2013.05.025>
- [4] D. Y. Shahriari, A. Barnabe, T. O. Mason, K. R. Poeppelmeier, A High-Yield Hydrothermal Preparation of  $\text{CuAlO}_2$ , *Inorg. Chem.* 2001;**40**:5734-5.

- [5] T. Dittrich, L. Dloczik, T. Guminskaya, M.C. Lux-Steiner, N. Grigorieva, I. Urban, "Photovoltage characterization of  $\text{CuAlO}_2$  crystallites", *Appl. Phys. Lett.*, 2004;**85**:742-4.
- [6] C. K. Ghosh, S. R. Popuri, T. U. Mahesh, K. K. Chattopadhyay, Preparation of nanocrystalline  $\text{CuAlO}_2$  through sol-gel rout, *J. Sol-Gel Sci. Technol.* 2010;**52**:75-81.
- [7] V. T. Kavitha, R. Jose, S. Ramakrishna, P. R. S. Wariar, J. Koshy, Combustion synthesis and characterization of  $\text{Ba}_2\text{NdSbO}_6$  nanocrystals, *Bull. Mater. Sci.* 2011;**34**:661–5.
- [8] G. E. Tobon-Zapata, S. B. Etcheverry, E. J. Baran, Vibrational spectrum of  $\text{KBi}(\text{C}_6\text{H}_4\text{O}_7) \cdot 3\text{H}_2\text{O}$ , the most simple species present in colloidal bismuth subcitrate, *Acta Farm. Bonaerense* 1997;**16**:145-50.